Time-resolved x-ray spectroscopies: Nonlinear response functions and Liouville-space pathways

Satoshi Tanaka,[1,2] Vladimir Chernyak,[1,3] and Shaul Mukamel[1]
[1]*Department of Chemistry, University of Rochester, Rochester, New York 14627*
[2]*College of Integrated Arts and Sciences, Osaka Prefecture University, Sakai 599-8531, Japan*
[3]*Process Engineering and Modeling, Corning, Inc., Corning, New York 14831*
(Received 14 December 2000; published 8 May 2001)

A systematic description of coherent ultrafast x-ray spectroscopies in terms of nonlinear response functions and susceptibilities is developed. Correlation-function expressions of charge and current densities provide a unified treatment and classification of information content of the various possible techniques and connect them with their optical counterparts. Applications to pump-probe and four-wave mixing measurements are discussed.

DOI: 10.1103/PhysRevA.63.063405 PACS number(s): 42.50.Hz

I. INTRODUCTION

With the advent of intense femtosecond coherent x-ray sources it is now feasible to carry out nonlinear spectroscopic studies of atoms, molecules, and condensed-phase materials in the x-ray region [1–16]. Most common are time-resolved x-ray diffraction (TRXD) experiments which directly probe structural changes induced by a visible or ultraviolet optical light pulse [1,2,4,8–10,14,15]. The time resolution of these techniques has evolved from msec [1] to 300 fsec [9]. Experiments have been carried out on crystals [4,8,9,14,17], powders [18], proteins [10], and liquids [8,18]. Experiments using time-resolved small angle x-ray diffraction have also been performed in large molecules and biomolecules [19]. X-ray absorption is another popular technique that has long been used in structure determination. Commonly used frequency domain absorption techniques include extended x-ray absorption fine structure (EXAFS) [20,21] or x-ray absorption near-edge spectroscopy (XANES) [21]. These have been recently extended to time-resolved pump-probe (XPP) spectroscopy where the absorption of an x-ray pulse is measured following an excitation by an optical pulse that prepares the system in a nonstationary state [3,8,11,12,16]. Experiments have been reported in the gas phase [12] and in liquids [8,11,16]. Frequency domain resonant x-ray emission was carried out in solids [22–25] and molecules [26–28], and has been the subject of extensive theoretical activity [29–33]. Resonant Auger emission spectroscopy is also a powerful probe for investigating the relaxation dynamics of the core excited state. Recently resonant Auger emission in the frequency domain has been extensively studied both theoretically [34,35] and experimentally [36–38].

In this article we develop a unified correlation-function theory for x-ray nonlinear spectroscopies. The most compact and general formulation of nonlinear optical spectroscopy is based on nonlinear response functions (NRF's) $S^{(n)}$, which are given by combinations of multitime correlation functions of the dipole operator [39]. Their frequency domain analogs, the nonlinear susceptibilities $\chi^{(n)}$, are used to describe long pulse experiments. NRF's provide the most natural meeting point of theory and experiment: They allow a systematic classification of the information content of various experiments and a unified description of many techniques. The NRF's are expressed as sums of *Liouville-space pathways*, which provide an intuitive picture for the time evolution of the density operator. NRF's also disentangle the roles of the laser pulses and the molecular response, and the signal is given by their convolution. In contrast, a wave-packet description based on a numerical solution of the wave function of the externally driven system requires a separate calculation for each spectroscopic technique.

This powerful nonlinear response formulation will be extended here to the x-ray regime. Several points of difference from optical techniques should be addressed. The response functions are nonlocal in time and space. In the optical regime the observed single-photon and multiphoton resonances are related to the *temporal* evolution and provide information about characteristic frequencies (energy levels of the system). The spatial dependence on the other hand, yields only a phase matching condition, e.g., the preferred wave vectors in four-wave mixing signals, but otherwise carries no useful physical information. The problem is that optical wavelengths are hundreds of nanometers and the atomic level spatial information is averaged out. One important difference between x-ray and optical spectroscopy is the spatial resolution offered by x-ray wavelengths in the 1–15 Å range, which is comparable to a bond distance or a lattice constant. Performing grating experiments with a combination of x-ray and optical beams should provide a direct and unambiguous probe of spatial coherence and motions of excitons and polaritons. This could not be achieved using optical transient gratings, despite considerable effort [40–42].

Another important aspect of x-ray techniques is that they probe the dynamics of charge and current densities rather than of the oscillator strength. Since charge distributions are directly related to chemical bonding and structure, molecular collisions and the creation and breaking of bonds can thus be monitored with femtosecond time resolution. TRXD and XPP spectroscopy can therefore directly probe electronic and nuclear motions and can be analyzed without resorting to any additional information. In contrast, we cannot obtain from optical nonlinear spectroscopy any information on the electronic and nuclear motions in real space without some prior knowledge and extensive simulations of potential energy surfaces and transition dipole matrix elements.

Since in the optical regime the wavelength is typically larger than all relevant molecular coherence sizes, one can treat the coupling of an optical field with the matter using the dipole approximation. It is then most convenient to use the multipolar Hamiltonian [39,43]. In contrast, the x-ray wavelength is shorter than the molecular coherence sizes, and the dipole approximation, which greatly simplifies the calculations, no longer holds. When using the multipolar Hamiltonian, we have to take into account the higher order contributions in the multipolar expansion, which makes the calculation much more complicated and harder to interpret. We therefore employ the minimal coupling $(\mathbf{p}\cdot\mathbf{A})$ Hamiltonian whereby the NRF's are expressed as multiple time correlation functions of charges and currents rather than of the dipole operator. The present formulation connects the x-ray and optical terminologies, and allows a systematic classification of various techniques according to different criteria such as nonlinear order (n), resonant vs off-resonant, time vs frequency domain etc., as is commonly done in the optical regime.

This paper is organized as follows. Starting with the minimal coupling Hamiltonian, general formal expressions for nonlinear spectroscopy are presented in Sec. II. The prescription for the calculation of NRF's to any order in the incoming fields and the connection with various signals and detection modes are given. Nonlinear spectroscopies in the purely x-ray region, such as x-ray pump-probe spectroscopy, multiwave mixing, and time- and frequency resolved emission spectroscopy are fascinating subjects, which can be readily formulated in terms of NRF's. Application to pump-probe spectroscopy which is a third order technique, is given in Sec. III. Our results are discussed in Sec. IV where the relation with previous treatments is discussed as well.

II. CORRELATION-FUNCTION EXPRESSIONS FOR NONLINEAR RESPONSE FUNCTIONS

We shall describe the radiation-matter coupling using the minimal coupling Hamiltonian which may be partitioned into three parts representing the matter (H_0), the radiation field (H_{rad}), and their interaction (H_{int}):

$$H_{tot}=H_0+H_{rad}+H_{int}, \tag{1a}$$

$$H_{rad}=\sum_{\mathbf{q}\lambda}\hbar\omega_{\mathbf{q}\lambda}b^{\dagger}_{\mathbf{q}\lambda}b_{\mathbf{q}\lambda}, \tag{1b}$$

$$H_{int}=-\int\hat{\mathbf{J}}(\mathbf{r})\cdot\hat{\mathbf{A}}(\mathbf{r},t)d\mathbf{r}. \tag{1c}$$

Here $b^{\dagger}_{\mathbf{q}\lambda}$ $(b_{\mathbf{q}\lambda})$ are the photon creation (annihilation) operators with energy $\hbar\omega_{\mathbf{q}\lambda}$, wave vector $\mathbf{q}$, and polarization λ. The vector potential $\hat{\mathbf{A}}(\mathbf{r},t)$ is given by

$$\hat{\mathbf{A}}(\mathbf{r},t)=\sum_{\mathbf{q}\lambda}c\frac{\epsilon_{\mathbf{q}}}{\omega_{\mathbf{q}}}\mathbf{e}_{\mathbf{q}\lambda}\{b_{\mathbf{q}\lambda}\exp[i(\mathbf{q}\cdot\mathbf{r}-\omega_{\mathbf{q}}t)]+b^{\dagger}_{\mathbf{q}\lambda}\exp[-i(\mathbf{q}\cdot\mathbf{r}-\omega_{\mathbf{q}}t)]\}, \tag{2}$$

where $\epsilon_{\mathbf{q}}=(2\pi\hbar\omega_{\mathbf{q}}/\Omega)^{1/2}$. $\hat{\mathbf{J}}(\mathbf{r})$ is the current density in the presence of the electromagnetic field,

$$\hat{\mathbf{J}}(\mathbf{r})=\hat{\mathbf{j}}(\mathbf{r})-\frac{e^2}{2mc}\hat{\mathbf{A}}(\mathbf{r},t)\hat{\sigma}(\mathbf{r}), \tag{3a}$$

$$\hat{\mathbf{j}}(\mathbf{r})\equiv\frac{e\hbar}{2mi}\{\hat{\psi}^{\dagger}(\mathbf{r})\nabla\hat{\psi}(\mathbf{r})-[\nabla\hat{\psi}(\mathbf{r})^{\dagger}]\hat{\psi}(\mathbf{r})\}, \tag{3b}$$

$$\hat{\sigma}(\mathbf{r})\equiv\hat{\psi}^{\dagger}(\mathbf{r})\hat{\psi}(\mathbf{r}), \tag{3c}$$

$\hat{\mathbf{j}}$ is the current density in the absence of $\hat{\mathbf{A}}(\mathbf{r},t)$, $\hat{\sigma}(\mathbf{r})$ is the charge density, and $\hat{\psi}^{\dagger}(\mathbf{r})$ $[\hat{\psi}(\mathbf{r})]$ are the field creation (annihilation) operators for the electron.

When the radiation field is treated classically, we need only consider the following Hamiltonian for the material system:

$$H=H_{mat}+H_{int}, \tag{4a}$$

$$H_{int}=H_1+H_2, \tag{4b}$$

$$H_1=-\int\mathbf{A}(\mathbf{r},t)\cdot\hat{\mathbf{j}}(\mathbf{r})d\mathbf{r}, \tag{4c}$$

$$H_2=\frac{e^2}{2mc}\int\mathbf{A}^2(\mathbf{r},t)\hat{\sigma}(\mathbf{r})d\mathbf{r}. \tag{4d}$$

From Eqs. (3), the expectation value of the current density at time t is given by

$$\mathbf{J}(\mathbf{r},t)=\langle\hat{\mathbf{j}}(\mathbf{r})\rangle_t-\frac{e^2}{2mc}\mathbf{A}(\mathbf{r},t)\langle\hat{\sigma}(\mathbf{r})\rangle_t, \tag{5a}$$

$$=\mathrm{Tr}[\hat{\mathbf{j}}(\mathbf{r})\rho(t)]-\frac{e^2}{2mc}\mathbf{A}(\mathbf{r},t)\mathrm{Tr}[\hat{\sigma}(\mathbf{r})\rho(t)], \tag{5b}$$

where $\rho(t)$ is the material density matrix. To describe the dynamics of the molecular system coupled to the radiation field, we expand $\rho(t)$ in powers of $\mathbf{A}$,

$$\rho(t)=\rho^{(0)}(t)+\rho^{(1)}(t)+\cdots, \tag{6}$$

where the nth order term $\rho^{(n)}(t)$ is obtained by expanding the Liouville equation pertubatively in H_{int}, i.e.,

$$\rho(t)=\sum_{n=0}^{\infty}\left(\frac{i}{\hbar}\right)^n\int d\mathbf{r}_n\cdots\int d\mathbf{r}_1\int dt_n\cdots\times\int dt_1\mathcal{G}(t_n)\mathcal{L}_{int}(\mathbf{r}_n,t-t_n)\mathcal{G}(t_n-1)\cdots\times\cdots\mathcal{G}(t_1)\mathcal{L}_{int}(\mathbf{r}_1,t-t_n-t_n-1\ldots-t_1)\rho(-\infty), \tag{7}$$

where $\mathcal{G}(t)$ is the Liouville-space Green function [39],

$$\mathcal{G}(t)\equiv\theta(t)e^{-(i/\hbar)\mathcal{L}_0t}. \tag{8}$$

In Eq. (8), $\theta(t)$ is a Heaviside step function and $\mathcal{L}_0$ is a Liouville operator which is defined as $\mathcal{L}_0\rho(t)=[H_0,\rho(t)]$. From Eqs. (4b)–(4d), the Liouville operator corresponding to H_{int} is

$$\mathcal{L}_{int}(\mathbf{r},t)\equiv -\mathcal{J}(\mathbf{r})\cdot\mathbf{A}(\mathbf{r},t) \tag{9a}$$

$$= -\mathcal{J}_0(\mathbf{r})\cdot\mathbf{A}(\mathbf{r},t)+\frac{e^2}{2mc}\mathcal{Z}(\mathbf{r})\mathbf{A}^2(\mathbf{r},t) \tag{9b}$$

$$=\mathcal{L}_1(\mathbf{r},t)+\mathcal{L}_2(\mathbf{r},t), \tag{9c}$$

where $\mathcal{J}$, $\mathcal{J}_0$, and $\mathcal{Z}$ are Liouville operators corresponding to $\hat{\mathbf{J}}$, $\hat{\mathbf{j}}$, and $\hat{\sigma}$, respectively.

Substituting Eq. (6) into Eq. (5b), we obtain the expansion of $\mathbf{J}(\mathbf{r},t)$ in powers of $\mathbf{A}$:

$$\mathbf{J}(\mathbf{r},t)=\sum_n \mathbf{J}^{(n)}(\mathbf{r},t), \tag{10}$$

where the nth order nonlinear current density is given by

$$\mathbf{J}^{(n)}(\mathbf{r},t)=\mathrm{Tr}[\hat{\mathbf{j}}(\mathbf{r})\rho^{(n)}]-\frac{e^2}{2mc}\mathbf{A}(\mathbf{r},t)\mathrm{Tr}[\hat{\sigma}(\mathbf{r})\rho^{(n-1)}]. \tag{11}$$

Spectroscopic signals are given by the NRF's $\mathsf{S}^{(n)}$ which are defined as the kernels of the time-ordered expansion of $\mathbf{J}^{(n)}(\mathbf{r},t)$,

$$\begin{aligned}J^{(n)}_{\lambda_s}(\mathbf{r},t)=&\int d\mathbf{r}_n\int d\mathbf{r}_{n-1}\cdots\int d\mathbf{r}_1\int dt_n\int dt_{n-1}\cdots\int dt_1\\ &\times\sum_{\lambda_1,\ldots,\lambda_n}\mathsf{S}^{(n)}_{\lambda_n,\ldots,\lambda_1\lambda_s}(\mathbf{r};\mathbf{r}_n,\mathbf{r}_{n-1},\ldots,t_n,t_{n-1},\ldots,t_1)A_{\lambda_n}(\mathbf{r}_n,t-t_n)\\ &\times A_{\lambda_{n-1}}(\mathbf{r}_{n-1},t-t_n-t_{n-1})\times\cdots\times A_{\lambda_1}(\mathbf{r}_1,t-t_n-t_{n-1}-\cdots-t_1).\end{aligned} \tag{12}$$

Upon substituting Eq. (7) and Eq. (9) into Eq. (5b) and comparing with Eq. (12), we can calculate the NRF's to any desired order. Closed formal expressions for the first, second, and third order response functions are given in Appendix A in terms of Liouville-space Green functions. In Appendix B these are recast as combinations of ordinary (Hilbert-space) correlation functions.

The expansion of the current in powers of the vector potential comes naturally when using the minimal coupling Hamiltonian. The connection with experimental signals is more clearly seen if we use different dynamical variables. Instead of $\mathbf{A}$, which depends on the gauge, we would like to use the transverse electric field $\mathbf{E}$, which is gauge invariant. They are related by

$$-\frac{d\mathbf{A}(\mathbf{r},t)}{dt}=\mathbf{E}(\mathbf{r},t). \tag{13}$$

Similarly, the polarization $\mathbf{P}$ is a more suitable material variable than the current $\mathbf{J}$, since it connects directly with the signal. In the multipolar Hamiltonian we have a microscopic expression for the polarization operator $\hat{\mathbf{P}}(\mathbf{r},t)$ [43]. This expression is nonlocal, depends on an arbitrary choice of origin and is not convenient to use except when the dipole approximation applies. The current and charge density operators used here are the natural variables since they are well defined and local. We can nevertheless express the final result using the polarization without defining a polarization operator. From the equation of continuity

$$\frac{\partial}{\partial t}\sigma(\mathbf{r},t)\equiv\frac{\partial}{\partial t}\mathrm{Tr}[\hat{\sigma}(\mathbf{r})\rho(t)]=-\boldsymbol{\nabla}\cdot\mathbf{J}(\mathbf{r},t) \tag{14}$$

and the definition of the polarization

$$\tilde{\mathbf{P}}(t)\equiv\int\mathbf{P}(\mathbf{r},t)d\mathbf{r}\equiv\int\mathbf{r}\sigma(\mathbf{r},t)d\mathbf{r}, \tag{15}$$

we obtain the relation between the current density and the polarization,

$$\frac{\partial}{\partial t}\tilde{\mathbf{P}}(t)=\int\mathbf{r}\frac{\partial}{\partial t}\sigma(\mathbf{r},t)d\mathbf{r}=-\int\mathbf{r}\boldsymbol{\nabla}\cdot\mathbf{J}(\mathbf{r},t)d\mathbf{r}=\int\mathbf{J}(\mathbf{r},t)d\mathbf{r}, \tag{16}$$

or

$$\mathbf{J}(\mathbf{r},t)=\frac{\partial\mathbf{P}(\mathbf{r},t)}{\partial t}. \tag{17}$$

We thus have

$$\mathbf{P}(\mathbf{r},t)=\int_{-\infty}^{t}d\tau\mathbf{J}(\mathbf{r},\tau). \tag{18}$$

The Maxwell equations then read

$$\boldsymbol{\nabla}\times\boldsymbol{\nabla}\times\mathbf{E}(\mathbf{r},t)+\frac{1}{c^2}\frac{\partial^2}{\partial t^2}\mathbf{E}(\mathbf{r},t)=-\frac{4\pi}{c^2}\frac{\partial^2\mathbf{P}(\mathbf{r},t)}{\partial t^2}. \tag{19}$$

Upon the substitution of Eqs. (13) and (18) in Eq. (12) we obtain a closed relation between $\mathbf{P}(\mathbf{r},t)$ and $\mathbf{E}(\mathbf{r},t)$ involving different response functions denoted $\mathsf{S}^{(n)}$:

$$P^{(n)}_{\lambda_s}(\mathbf{r},t)=\int d\mathbf{r}_n\int d\mathbf{r}_{n-1}\cdots\int d\mathbf{r}_1\int dt_n\int dt_{n-1}\cdots\int dt_1$$
$$\times\sum_{\lambda_1,\ldots,\lambda_n}\mathcal{S}^{(n)}_{\lambda_n,\ldots,\lambda_1\lambda_s}(\mathbf{r};\mathbf{r}_n,\mathbf{r}_{n-1},\ldots,t_n,t_{n-1},\ldots t_1)\cdot E_{\lambda_n}(\mathbf{r}_n,t-t_n)\cdot E_{\lambda_{n-1}}(\mathbf{r}_{n-1},t-t_n-t_{n-1})\times\cdots$$
$$\times E_{\lambda_1}(\mathbf{r}_1,t-t_n-t_{n-1}-\cdots-t_1). \tag{20}$$

The relation between $\mathcal{S}^{(n)}$ and $\mathsf{S}^{(n)}$ is more compact in the frequency domain, when using susceptibilities (rather than response functions) and is presented in Appendix C. The relation between the two types of response function in the time domain is simplified considerably when the slowly varying amplitude approximation holds for the fields. We shall expand the field as

$$E(\mathbf{r},t)=\sum_j E_j(t)\exp(i\mathbf{k}_j\cdot\mathbf{r}-i\omega_j t)+\text{c.c.} \tag{21}$$

The wave vectors and frequencies for each field are $\mathbf{k}_j\omega_j$. Since the field amplitudes E_j change on a slower time scale than the optical periods $2\pi/\omega_j$, this is known as the slowly varying amplitude approximation [44], and we get

$$\mathcal{S}^{(n)}(\mathbf{r};r_n,\ldots,r_1,t_n,\ldots,t_1)$$
$$=\frac{i^{1-n}}{\omega_1\omega_2\cdots\omega_n\omega_s}\mathsf{S}^{(n)}(\mathbf{r};r_n,r_1,\ldots,t_n,\ldots,t_1), \tag{22}$$

where $\omega_s=\pm\omega_1\pm\omega_2\pm\cdots\pm\omega_n$.

It should be noted that although we treated the optical field classically our results represent the response to the actual Maxwell field rather than to the external field. This approach does not treat rigorously the radiative corrections to the response functions, but treats them at a mean field level by including the field irradiated by the material in the actual field. This issue is discussed in detail in [45–47].

To calculate specific signals we expand the polarization in $\mathbf{k}$ space,

$$\mathbf{P}^{(n)}(\mathbf{r},t)=\sum_s \mathbf{P}^{(n)}(\mathbf{k}_s,t)\exp(i\mathbf{k}_s\cdot\mathbf{r}), \tag{23}$$

where $\mathbf{k}_s$ is any combination $\mathbf{k}_s=\pm\mathbf{k}_1\pm\mathbf{k}_2\pm\cdots\pm\mathbf{k}_n$. Various detection modes are possible. The homodyne detected signal is given by

$$W_s=\int |P^{(n)}(\mathbf{k}_s,t)|^2dt, \tag{24}$$

whereas heterodyne detection gives

$$W_s=\omega_s\,\mathrm{Im}\int E^*_{L_s}(t)P^{(n)}(\mathbf{k}_s,t)dt. \tag{25}$$

III. APPLICATION TO PUMP-PROBE X-RAY SPECTROSCOPY

Pump-probe is the simplest nonlinear optical technique. The system is subjected to two pulses: the pump pulse excites the system into a nonstationary state which is then monitored by the change in the absorption of a second pulse, the probe, which comes at variable delay τ with respect to the pump. The pump may be either a visible pulse that prepares the system in an electronically excited state, inducing various dynamical processes such as vibrational excitation, bond breaking, etc., or a resonant x-ray pulse that induces inner-core excitations. In the following we assume a resonant x-ray probe. The incoming field is

$$E(\mathbf{r},t)=E_1(t+\tau)e^{i(\mathbf{k}_1\cdot\mathbf{r}-\omega_1 t)}+E_2(t)e^{i(\mathbf{k}_2\cdot\mathbf{r}-\omega_2 t)}+\text{c.c.}, \tag{26}$$

where $E_1(t+\tau)$ is the temporal envelope of the optical pump field peaked at time $t=-\tau$, while $E_2(t)$ is the x-ray probe field peaked at $t=0$. The pump-probe signal is generated in the direction of the probe, which constitutes an intrinsic heterodyne detection $\mathbf{k}_s=\mathbf{k}_1-\mathbf{k}_1+\mathbf{k}_2$ [39] and in the slowly varying amplitude approximation is given by

$$W_{PP}(\mathbf{k}_1\omega_s,\mathbf{k}_2\omega_2;\tau)$$
$$\propto\omega_2\int d\mathbf{r}\int dt\,\mathrm{Im}[E_2^*(t)P^{(3)}(\mathbf{r},t)e^{-i(\mathbf{k}_2\cdot\mathbf{r}-\omega_2 t)}]$$
$$=\omega_2\,\mathrm{Im}\int dtE_2(t)P^{(3)}(\mathbf{k}_s,t)$$
$$\propto-\frac{\omega_2}{2}\int d\mathbf{r}\int dt\,\mathrm{Im}[A_2^*(t)J^{(3)}(\mathbf{r},t)e^{-i(\mathbf{k}_2\cdot\mathbf{r}-\omega_2 t)}]. \tag{27}$$

We further assume that the time delay τ is long to ensure a sequential (pump-first) time ordering.

Since all fields are resonant, we can retain only the first term in the coupling Eq. (4c) and we neglect Eq. (4d). We note that the field-matter interaction contains both linear and bilinear terms in the vector potential. Generally both terms are important. The linear term is proportional to the electron velocity and therefore dominates the interaction in the resonance region where electron motions are fast. On the other hand, for high frequency radiation fields the electron velocities are low and the interaction is dominated by the bilinear term, which does not include the electron velocity. In the

dipole approximation utilization of a certain sum rule makes the interaction linear in the electric field. This can be alternatively explained as follows. Performing a gauge transformation to the multipolar gauge [48], the interaction becomes linear in the electric field (electric terms) and linear and bilinear in the vector potential (magnetic terms). If the latter can be neglected (e.g., when the dipole approximation holds) the interaction becomes linear. Adopting this language the interaction becomes linear by means of the gauge transformation. These two explanations are equivalent since the aforementioned sum rule is the consequence of gauge invariance. We emphasize that the system-field interaction can be represented as a linear coupling with the electric field only if we neglect the magnetic terms in the multipolar gauge. In general the interaction involves the vector potential as well and includes linear and bilinear terms. We also note that at low frequencies the response with respest to the vector potential tends to zero and the response with respect to the electric field becomes finite, which means that the apparent zero frequency poles in the right-hand side of Eq. (22) must cancel once the response is properly calculated.

Substituting Eq. (A5) into Eq. (27) and replacing the vector potential with the electric field, we obtain

$$W_{PP}(\mathbf{k}_1\omega_1,\mathbf{k}_2\omega_2;\tau)=\frac{1}{2}\frac{1}{\omega_1^2\omega_2}\mathrm{Re}\int d\mathbf{r}\int d\mathbf{r}_3\int d\mathbf{r}_2\int d\mathbf{r}_1\int dt\int dt_3\int dt_2\int dt_1(E_1^*(t-t_3-t_2-t_1+\tau)E_1(t-t_3-t_2$$
$$+\tau)E_2(t-t_3)E_2^*(t)\exp[-i\mathbf{k}_1\cdot(\mathbf{r}_1-\mathbf{r}_2)+i\mathbf{k}_2\cdot(\mathbf{r}_3-\mathbf{r})]\exp[-i\omega_1t_1+i\omega_2t_3]\{R_1(\mathbf{r};\mathbf{r}_3\mathbf{r}_2\mathbf{r}_1t_3t_2t_1)$$
$$+R_3(\mathbf{r};\mathbf{r}_3\mathbf{r}_2\mathbf{r}_1t_3t_2t_1)\}+E_1(t-t_3-t_2-t_1+\tau)E_1^*(t-t_3-t_2+\tau)E_2(t-t_3)E_2^*(t)$$
$$\times\exp[i\mathbf{k}_1\cdot(\mathbf{r}_1-\mathbf{r}_2)+i\mathbf{k}_2(\mathbf{r}_3-\mathbf{r})]\exp[i\omega_1t_1+i\omega_2t_3]\cdot\{R_2(\mathbf{r};\mathbf{r}_3\mathbf{r}_2\mathbf{r}_1t_3t_2t_1)+R_4(\mathbf{r};\mathbf{r}_3\mathbf{r}_2\mathbf{r}_1t_3t_2t_1)\}). \tag{28}$$

Each R_j represents a distinct Liouville-space pathway contribution to the response, as shown in Fig. 1. The corresponding correlation-function expressions are

$$R_1=-\langle\hat{j}(\mathbf{r}_1,0)\hat{j}(\mathbf{r},t_1+t_2+t_3)\hat{j}(\mathbf{r}_3,t_1+t_2)\hat{j}(\mathbf{r}_2,t_1)\rangle, \tag{29a}$$

$$R_2=-\langle\hat{j}(\mathbf{r}_2,t_1)\hat{j}(\mathbf{r},t_1+t_2+t_3)\hat{j}(\mathbf{r}_3,t_1+t_2)\hat{j}(\mathbf{r}_1,0)\rangle, \tag{29b}$$

$$R_3=\langle\hat{j}(\mathbf{r}_1,0)\hat{j}(\mathbf{r}_2,t_1)\hat{j}(\mathbf{r},t_1+t_2)\hat{j}(\mathbf{r}_3,t_1+t_2+t_3)\rangle, \tag{29c}$$

$$R_4=\langle\hat{j}(\mathbf{r},t_1+t_2+t_3)\hat{j}(\mathbf{r}_3,t_1+t_2)\hat{j}(\mathbf{r}_2,t_1)\hat{j}(\mathbf{r}_1,0)\rangle. \tag{29d}$$

In the above expressions, $\hat{j}(\mathbf{r},t)$ are the Heisenberg representation. [See Eq. (B4)].

Alternative expressions for these correlation functions are given in Appendix D.

Let us consider an experiment conducted with an optical pump and x-ray probe. g (g'), e (e'), and f stand for the vibronic eigenstates of the ground, excited, and final electronic states, respectively. These correlation functions can also be recast in the form of sums over eigenstates:

$$R_1=-\sum_{gee'f}P(g)j_{e'f}(\mathbf{r})j_{fe}(\mathbf{r}_3)j_{eg}(\mathbf{r}_2)j_{e'g}^*(\mathbf{r}_1)I_{fe'}(t_3)I_{ee'}(t_2)I_{ge'}(t_1), \tag{30a}$$

$$R_2=-\sum_{gee'f}P(g)j_{e'f}(\mathbf{r})j_{fe}(\mathbf{r}_3)j_{e'g}^*(\mathbf{r}_2)j_{eg}(\mathbf{r}_1)I_{fe'}(t_3)I_{ee'}(t_2)I_{eg}(t_1), \tag{30b}$$

$$R_3=\sum_{gg'ef}P(g)j_{g'f}(\mathbf{r})j_{fg}(\mathbf{r}_3)j_{g'e}^*(\mathbf{r}_2)j_{eg}^*(\mathbf{r}_1)I_{fg'}(t_3)I_{gg'}(t_2)I_{ge}(t_1), \tag{30c}$$

$$R_4=\sum_{gg'ef}P(g)j_{gf}(\mathbf{r})j_{fg'}(\mathbf{r}_3)j_{g'e}(\mathbf{r}_2)j_{eg}(\mathbf{r}_1)I_{fg}(t_3)I_{g'g}(t_2)I_{eg}(t_1). \tag{30d}$$

$I_{\nu\nu'}(t)$ is an auxiliary function denoting matrix elements of the Green function $\mathcal{G}(t)$ [Eq. (8)], i.e.,

$$I_{\nu\nu'}(t) \equiv \theta(t)\exp[-i\omega_{\nu\nu'}t-\Gamma_{\nu\nu'}t], \tag{31}$$

where $\hbar\omega_{\nu\nu'}\equiv\epsilon_\nu-\epsilon_{\nu'}$ is the transition frequency, and $\Gamma_{\nu\nu'}$ is the dephasing rate of the $\nu\nu'$ transition. As is clearly seen from Fig. 1, there are contributions from the ground state population (R_3 and R_4) as well as from the optically excited state population (R_1 and R_2).

Since we assume that the pump and the probe are temporally well separated, we can split Eqs. (28) into two parts representing the actions of the pump and the probe. This is known as the doorway window picture [39]. The signal may then be expressed as the current density correlation function with respect to the nonequilibrium density operator $\tilde{\rho}^{(2)}(t)$:

$$\begin{aligned} W_{PP}=&\frac{1}{2}\frac{1}{\omega_1^2\omega_2}\mathrm{Re}\int d\mathbf{r}\int d\mathbf{r}_3\int dt\int dt_3 \\ &\times E_2^*(t)E_2(t-t_3)\exp[i\mathbf{k}_2\cdot(\mathbf{r}_3-\mathbf{r})+i\omega_2 t_3] \\ &\times \mathrm{Tr}[\hat{j}(\mathbf{r},t)\hat{j}(\mathbf{r}_3,t-t_3)\tilde{\rho}^{(2)}(t-t_3)]. \end{aligned} \tag{32}$$

All the information about the excitation is now carried by $\tilde{\rho}^{(2)}(t-t_3)$, which is given by

$$\begin{aligned} \tilde{\rho}^{(2)}(t-t_3)=&-\frac{1}{\hbar^2}\int d\mathbf{r}_2\int d\mathbf{r}_1\int dt_2\int dt_1 \\ &\times[\hat{j}(\mathbf{r}_2,t-t_2-t_3),[\hat{j}(\mathbf{r}_1,t-t_1-t_2-t_3),\rho(-\infty)]] \\ &\times E_1(\mathbf{r}_1,t-t_1-t_2-t_3)E_1(\mathbf{r}_2,t-t_2-t_3). \end{aligned} \tag{33}$$

This density operator represents the molecular state at time $t-t_3$ following the pump excitation. The ordinary (stationary) x-ray absorption spectrum is obtained by simply replacing $\tilde{\rho}^{(2)}(t)$ with the ground state density matrix $\rho(-\infty)$ in Eq. (32).

To examine the role of spatial coherence in pump-probe spectroscopy, we shall expand Eq. (32) in a localized basis set. The field operators $\hat{\psi}(\mathbf{r})$ and $\hat{\psi}^\dagger(\mathbf{r})$ in Eqs. (3) can then be represented by

$$\hat{\psi}(\mathbf{r})=\sum_{\alpha,l}\varphi_\alpha(\mathbf{r}-\mathbf{R}_l)a_\alpha(l), \quad \hat{\psi}^\dagger(\mathbf{r})=\sum_{\alpha,l}\varphi_\alpha^*(\mathbf{r}-\mathbf{R}_l)a_\alpha^\dagger(l), \tag{34}$$

where $a_\alpha(l)$ $[a_\alpha^\dagger(l)]$ are annihilation (creation) operators for the electron in the atomic state α and at a site l, and $\varphi_\alpha(\mathbf{r}-\mathbf{R}_l)$ is the corresponding atomic wave function. Substituting these into Eq. (3b), we obtain

$$\begin{aligned} &\int d\mathbf{r}\hat{j}(\mathbf{r})\exp[-i\mathbf{R}\cdot\mathbf{r}] \\ &=\frac{e}{m}\sum_{l,l'}\sum_{\alpha\alpha'}\exp[-i\mathbf{k}\cdot\mathbf{R}_l]\frac{1}{2} \\ &\times\int d\mathbf{r}\left\{a_\alpha^\dagger(l)a_{\alpha'}(l')\varphi_\alpha^*(\mathbf{r}-\mathbf{R}_l)\left(\frac{\hbar}{i}\nabla\varphi_{\alpha'}(\mathbf{r}-\mathbf{R}_{l'})\right)\right. \\ &\left.+a_{\alpha'}^\dagger(l')a_\alpha(l)\left(-\frac{\hbar}{i}\nabla\varphi_{\alpha'}^*(\mathbf{r}-\mathbf{R}_{l'})\right)\varphi_\alpha(\mathbf{r}-\mathbf{R}_l)\right\}. \end{aligned} \tag{35}$$

Without loss of generality, we can assume that each atomic site has a single core state denoted c. Invoking the rotating-wave approximation (RWA) we can then take α' as a core state denoted c. Taking into account the strong localization of the core wave function $\varphi_c(\mathbf{r}-\mathbf{R}_l)$ around the site l, we obtain

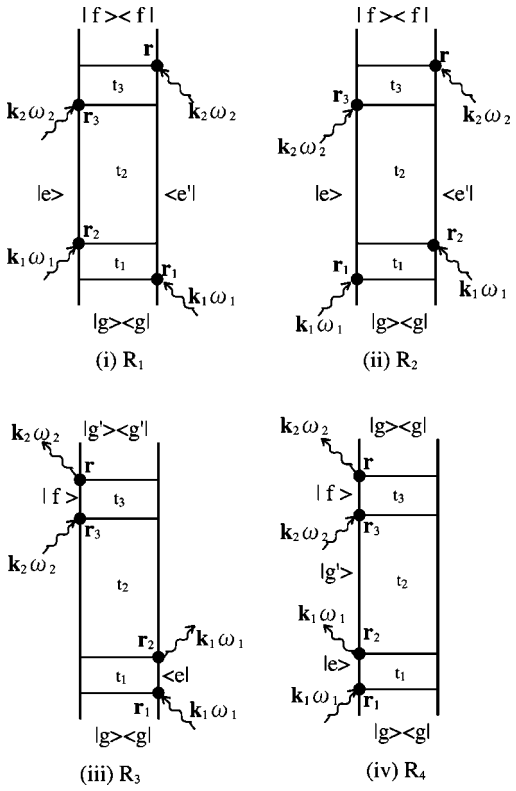

FIG. 1. Pictorial representation of the Liouville-space pathways contributing to the TRXA. Each pathway corresponds to the NRF of R_j ($j=1$–4) in Eqs. (32). g (or g'), e (or e'), and f stand for vibronic eigenstates belonging to the ground, the excited, and the final electronic states, respectively. For optical pump/x-ray probe, e (or e') stand for vibronic eigenstates of the optically excited state and f for those of a core excited state. For x-ray pump/x-ray probe, e (or e') represent vibronic eigenstates of the core excited state, and f represents those of either a doubly core excited state or the ground state.

$$\int d\mathbf{r}\hat{j}(\mathbf{r})\exp(-i\mathbf{k}\cdot\mathbf{r}) = \sum_l \sum_\alpha \exp(-i\mathbf{k}\cdot\mathbf{R}_l) j_{\alpha c}\{a_\alpha^\dagger(l)a_c(l)+\text{H.c.}\}, \tag{36}$$

where $j_{\alpha c}$ is the atomic current density matrix element between the core state c and the high energy state α:

$$j_{\alpha c} = \frac{e}{m}\text{Re}\int d\mathbf{r}\varphi_\alpha^*(\mathbf{r})\left(\frac{\hbar}{i}\nabla\varphi_c(\mathbf{r})\right). \tag{37}$$

Substituting Eq. (36) into Eq. (32), we can write

$$\int d\mathbf{r}\int d\mathbf{r}_3 e^{i\mathbf{k}_2(\mathbf{r}_3-\mathbf{r})}\text{Tr}[\hat{j}(\mathbf{r},t)\hat{j}(\mathbf{r}_3,t-t_3)\tilde{\rho}^{(2)}(t-t_3)] = \sum_{ll'}\sum_{\alpha\alpha'} j_{\alpha c}j_{\alpha' c}e^{i\mathbf{k}_2\cdot(\mathbf{R}_l-\mathbf{R}_{l'})} \times \text{Tr}[e^{(i/\hbar)H_0 t}a_c^\dagger(l)a_\alpha(l)e^{-(i/\hbar)H_0 t_3}a_{\alpha'}^\dagger(l')a_c(l') \times e^{-(i/\hbar)H_0(t-t_3)}\tilde{\rho}^{(2)}(t-t_3)]. \tag{38}$$

The charge transfer of the core states between the different atomic sites is usually neglected. Under this condition, we retain only the $l=l'$ terms in Eq. (37), so that the pump-probe signal can be represented as the sum of the absorption spectrum for each atomic site:

$$W_{PP} = \sum_l W_{PP}^l, \tag{39}$$

where W_{PP}^l stands for the atomic absorption spectrum for the lth site:

$$W_{PP}^l = \frac{1}{2}\frac{1}{\omega_1^2\omega_2}\text{Re}\int dt\int dt_3 E_2^*(t)E_2(t-t_3)\exp[i\omega_2 t_3] \times \text{Tr}[\hat{j}_l^\dagger(t)\hat{j}_l(t-t_3)\tilde{\rho}^{(2)}(t-t_3)]. \tag{40}$$

In Eq. (39), $\hat{j}_l(t)$ is the atomic current density operator in the Heisenberg representation ,

$$\hat{j}_l \equiv \sum_\alpha j_{\alpha c}a_\alpha^\dagger(l)a_c(l). \tag{41}$$

As a result of neglecting charge transfer of the core states between different sites there is no spatial correlation in Eq. (40), and the signal is simply expressed as a sum of atomic absorption spectra. Therefore the x-ray pump-probe spectrum does not produce information on the spatial coherence of core hole states and the signal has been traditionally interpreted using a single site model.

Equation (28) describes both time-resolved EXAFS and XANES techniques. In EXAFS the core electron is excited to the high energy continuum and the photoelectron is scattered by the surrounding atoms. EXAFS is attributed to the interference of the outgoing and backscattering waves of the photoelectron from a core excited atom and it has been interpreted in terms of the multiple scattering of the photoelectron from the surrounding atoms [20]. The Fourier transform of the signal as a function of the wave number of the photoelectron directly gives us the radial distribution function around the core excited atom. It can therefore probe the local structure around the selected core excited atom [20,21]. Thus time-resolved EXAFS has become a powerful tool for investigating optically-induced local structural changes of materials such as molecules in liquids, amorphous compounds, and crystals [8,11,12].

On the other hand, in XANES the core electron is excited to a bound state just below the ionization threshold. XANES spectra typically consist of several well-resolved lines corresponding to core electron transitions to unoccupied molecular orbitals or to core exciton states in the condensed phase [21,49–52]. While EXAFS can be interpreted by the solution of a single body problem, in order to interpret the origin of these spectral features it is necessary to take into account the many-body effects of electrons due to the attractive core hole potential, which causes the charge redistribution of the electrons in the core excited state [49–52]. These distinct resonance states of the core excited state lead to the chracteristic resonant enhancement in nonlinear spectroscopy in the x-ray region, such as resonant x-ray emission and x-ray pump and x-ray probe spectroscopy, which is essential for investigating the relaxation dynamics of the core excited states. This will be studied in a forthcoming paper.

IV. DISCUSSION

In this paper we have developed a unified formalism that establishes the formal connection between various nonlinear spectroscopies in the x-ray region. Starting with the minimal coupling Hamiltonian, we expanded the density operator in powers of the electric fields, and obtained formal expressions for the various signals in terms of the NRF's. These in turn are represented as combinations of multiple-time correlation functions of the current and the charge density operators. Since the NRF carries all the relevant material information, it can be applied to a broad range of nonlinear spectroscopies, which differ in the temporal sequences of pulses as well as in their frequencies and wave vectors.

Time-resolved x-ray diffraction is formulated in a similar way in Appendix E. The TRXD signal can be recast in the form

$$W_{TRXD} = -2\frac{1}{\omega_i^2}\text{Re}\int d\mathbf{r}\int d\mathbf{r}_3\int dt\int dt_3 E_i^*(t)E_i(t-t_3) \times \exp[i\Delta\mathbf{k}\cdot(\mathbf{r}-\mathbf{r}_3)-i\Delta\omega t_3] \times \text{Tr}[\hat{\sigma}(\mathbf{r},t)\hat{\sigma}(\mathbf{r}_3,t-t_3)\tilde{\rho}^{(2)}(t-t_3)], \tag{42}$$

which is formally very similar to Eq. (40). In Eq. (42), $\Delta\mathbf{k} \equiv \mathbf{k}_s-\mathbf{k}_i$ is the x-ray scattering wave vector and $\Delta\omega\equiv\omega_s$

$-\omega_i$ is the energy loss. Equation (42) represents an ordinary x-ray scattering intensity provided we replace $\tilde{\rho}^{(2)}(t-t_3)$ with the ground state density operator $\rho(-\infty)$. When $\Delta\omega=0$ it represents ordinary x-ray diffraction, but for $\Delta\omega\neq 0$ it gives inelastic scattering processes. Equation (42) shows that TRXD is obtained as the convolution of the Fourier transform of the optically induced dynamical strucure factor with the x-ray probe pulse. The optically induced dynamical structure factor can also be measured by time-resolved electron energy loss spectroscopy [53,54].

There have been a large number of theoretical and experimental studies of resonant frequency domain x-ray scattering in the condensed phase and on single molecules [26,27,29–32,55–63]. Except for a few studies [30,55,64,65], almost all of these theories are based on the Kramers-Heisenberg expression. The x-ray scattering intensity is proportional to the incident x-ray intensity and technically the process belongs to the domain of linear spectroscopy. However from a theoretical viewpoint this process may be described using third order NRF's, and it is therefore closely related to $\chi^{(3)}$ and can be thought of as a nonlinear spectroscopy [39]. In order to clarify the role of temporal and spatial coherence in resonant x-ray scattering processes, it is highly desirable to formulate them using NRF's which can be interpreted using Liouville-space pathways. The contributions from the fluorescence and coherent Raman components can be clearly separated using this approach.

Phenomenological theories of TRXD and XPP were developed in analogous ways to those for stationary x-ray diffraction and x-ray absorption processes [2,3,5]. The signals are simply given by correlation functions of the charge density and the current density, respectively, where the expectation value is taken with respect to the time-evolved state after the optical pump pulse excitation rather than for the ground state. The approach is based on a wave-function description where transition amplitudes are calculated first and the products of such amplitudes are subsequently summed to obtain the signal. Liouville space has many advantages over wave-function-based descriptions. Wave functions do not have a classical counterpart, making it hard to develop a simple physical interpretation for the signal [39]. In the perturbative expansion of the wave function time variables are not fully ordered and have a much less clear physical meaning, and it is difficult to assess the relationships among different nonlinear spectroscopies. In addition, dephasing processes cannot be introduced unless the wave function describes the entire system, which is impractical for large systems.

Even though the intensity of the TRXD signal is proportional to the incident x-ray beam, it is represented in the same way as in pump-probe spectroscopy, which is regarded as an optical pump and x-ray probe nonlinear spectroscopy. The similarity of the two becomes particularly clear when the NRF's are depicted in Liouville space.

Despite the similarity of the Liouville-space pathways for TRXD and XPP, spectroscopies there is an important difference between these two spectroscopies with regard to spatial coherence. In TRXD, spatial coherence is detected through the optically induced dynamical structure factor. On the other hand, due to the strongly localized nature of the core states, spatial coherence is not important in the pump-probe technique.

By representing both TRXD and XPP techniques using NRF's in Liouville space, it becomes clear that we have to take into account contributions from excited state (R_1 and R_2) as well as ground state (R_3 and R_4) populations. The latter contribution was neglected in earlier studies which assumed a strong field molecular π-pulse excitation [2,3]. Strong field optical experiments are harder to interpret due to complex photochemistry and the involvement of a large number of high excited electronic states. Ground and excited state contributions can be separated using the coherent Raman scattering technique in the purely x-ray region, which is a nonlinear four-wave mixing x-ray spectroscopy. Nonlinear spectroscopies in the x-ray region should provide powerful probes for investigating electronic states, relaxation processes, and energy transfer mechanisms with high spatial resolution. The temporal and spatial coherence in the molecular excited states could be directly probed as well. Formal expressions for these techniques will be presented in a forthcoming paper.

The absence of spatial coherence in the pump-probe spectrum is attributed to the fact that the x-ray absorption is represented by two-point correlation functions. As a result of neglecting the transfer of core states between different sites the two site indices for the core state must be the same. On the other hand, since the time- and frequency-resolved x-ray emission spectroscopy and x-ray pump x-ray probe spectroscopy are represented by four-point correlation functions they contain direct signatures of spatial coherence of the core hole states. In these spectroscopies, the single site model is no longer applicable [26,56]. The theory of these interesting purely x-ray nonlinear spectroscopies will be presented in a forthcoming paper.

ACKNOWLEDGMENTS

This work was partly supported by a Grant-in-Aid for Scientific Research from the Ministry of Education, Science, Sports, and Culture in Japan. We gratefully acknowledge the support of the National Science Foundation and the Petroleum Research Fund administered by the American Chemical Society.

APPENDIX A: LIOUVILLE-SPACE EXPRESSIONS FOR THE NRF

In this appendix we present expressions for the first, second, and third order nonlinear current density. These are obtained by substituting the perturbative expansion of the density matrix [Eq. (7)] into Eq. (11).

The first order current density is given by

$$J^{(1)}_{\lambda_s}(\mathbf{r},t)=\sum_{\lambda_1}\int d\mathbf{r}_1\int_0^\infty dt_1 \mathrm{S}^{(1)}_{\lambda_1\lambda_s}(\mathbf{r};\mathbf{r}_1 t_1)A_{\lambda_1}(\mathbf{r}_1,t-t_1), \tag{A1}$$

where the linear response function is written as

$$\mathsf{S}^{(1)}_{\lambda_1\lambda_s}(\mathbf{r};\mathbf{r}_1 t_1)=\frac{i}{\hbar}\langle\langle \hat{j}_{\lambda_s}(\mathbf{r})|\mathcal{G}(t_1)\mathcal{J}_{0\lambda_1}(\mathbf{r}_1)|\rho(-\infty)\rangle\rangle-\frac{e^2}{2mc}\langle\langle \hat{\sigma}(\mathbf{r})|\rho(-\infty)\rangle\rangle \times\delta(\mathbf{r}-\mathbf{r}_1)\,\delta(t_1)\,\delta_{\lambda_s\lambda_1}. \tag{A2}$$

The second order nonlinear current density is given by

$$J^{(2)}_{\lambda_s}(\mathbf{r},t)=\sum_{\lambda_1\lambda_2}\int d\mathbf{r}_2\int d\mathbf{r}_1\int dt_2\int dt_1\,\mathsf{S}^{(2)}_{\lambda_2\lambda_1\lambda_s}(\mathbf{r};\mathbf{r}_2\mathbf{r}_1 t_2 t_1)A_{\lambda_2}(\mathbf{r}_2,t-t_2)A_{\lambda_1}(\mathbf{r}_1,t-t_2-t_1), \tag{A3}$$

where the second order NRF is

$$\mathsf{S}^{(2)}_{\lambda_2\lambda_1\lambda_s}(\mathbf{r};\mathbf{r}_2\mathbf{r}_1 t_2 t_1)=\left(\frac{i}{\hbar}\right)^2\langle\langle \hat{j}_{\lambda_s}(\mathbf{r})|\mathcal{G}(t_2)\mathcal{J}_{0\lambda_2}(\mathbf{r}_2)\mathcal{G}(t_1)\mathcal{J}_{0\lambda_1}(\mathbf{r}_1)|\rho(-\infty)\rangle\rangle+\frac{e^2}{2mc}\left(-\frac{i}{\hbar}\right)\{\langle\langle \hat{j}_{\lambda_s}(\mathbf{r})|\mathcal{G}(t_1)\mathcal{Z}(\mathbf{r}_1)|\rho(-\infty)\rangle\rangle \times\delta_{\lambda_2\lambda_1}\delta(\mathbf{r}_2-\mathbf{r}_1)\,\delta(t_1)+\langle\langle \hat{\sigma}(\mathbf{r})|\mathcal{G}(t_1)\mathcal{J}_{0\lambda_1}(\mathbf{r}_1)|\rho(-\infty)\rangle\rangle\,\delta_{\lambda_2\lambda_s}\delta(\mathbf{r}-\mathbf{r}_2)\,\delta(t_2)\}. \tag{A4}$$

The third order nonlinear current density is given by

$$J^{(3)}_{\lambda_s}(\mathbf{r},t)=\sum_{\lambda_3\lambda_2\lambda_1}\int d\mathbf{r}_3\int d\mathbf{r}_2\int d\mathbf{r}_1\int dt_3\int dt_2\int dt_1\,\mathsf{S}^{(3)}_{\lambda_3\lambda_2\lambda_1\lambda_s}(\mathbf{r};\mathbf{r}_3\mathbf{r}_2\mathbf{r}_1 t_3 t_2 t_1) \times A_{\lambda_3}(\mathbf{r}_3,t-t_3)A_{\lambda_2}(\mathbf{r}_2,t-t_3-t_2)A_{\lambda_1}(\mathbf{r}_1,t-t_3-t_2-t_1), \tag{A5}$$

where the third order NRF is written as

$$\begin{aligned}\mathsf{S}^{(3)}_{\lambda_3\lambda_2\lambda_1\lambda_s}(\mathbf{r};\mathbf{r}_3\mathbf{r}_2\mathbf{r}_1 t_3 t_2 t_1)=(-)&\left(-\frac{i}{\hbar}\right)^3\langle\langle \hat{j}_{\lambda_s}(\mathbf{r})|\mathcal{G}(t_3)\mathcal{J}_{0\lambda_3}(\mathbf{r}_3)\mathcal{G}(t_2)\mathcal{J}_{0\lambda_2}(\mathbf{r}_2)\mathcal{G}(t_1)\mathcal{T}_{0\lambda_1}(\mathbf{r}_1)|\rho(-\infty)\rangle\rangle\\ &+\left(-\frac{e^2}{2mc}\right)\left(-\frac{i}{\hbar}\right)^2\{\langle\langle \hat{j}_{\lambda_s}(\mathbf{r})|\mathcal{G}(t_3)\mathcal{Z}(\mathbf{r}_3)\mathcal{G}(t_1)\mathcal{J}_{0\lambda_1}(\mathbf{r}_1)|\rho(-\infty)\rangle\rangle\,\delta_{\lambda_2\lambda_3}\delta(\mathbf{r}_2-\mathbf{r}_3)\,\delta(t_2)\\ &+\langle\langle \hat{j}_{\lambda_s}(\mathbf{r})|\mathcal{G}(t_3)\mathcal{J}_{0\lambda_3}(\mathbf{r}_3)\mathcal{G}(t_2)\mathcal{Z}(\mathbf{r}_2)|\rho(-\infty)\rangle\rangle\,\delta_{\lambda_2\lambda_1}\delta(\mathbf{r}_2-\mathbf{r}_1)\,\delta(t_1)\\ &+\langle\langle \hat{\sigma}(\mathbf{r})|\mathcal{G}(t_2)\mathcal{J}_{0\lambda_2}(\mathbf{r}_2)\mathcal{G}(t_1)\mathcal{J}_{0\lambda_1}(\mathbf{r}_1)|\rho(-\infty)\rangle\rangle\,\delta_{\lambda_3\lambda_s}\delta(\mathbf{r}-\mathbf{r}_3)\,\delta(t_3)\}-\left(\frac{e^2}{2mc}\right)^2\left(-\frac{i}{\hbar}\right)\\ &\times\langle\langle \hat{\sigma}(\mathbf{r})|\mathcal{G}(t_2)\mathcal{Z}(\mathbf{r}_2)|\rho(-\infty)\rangle\rangle\,\delta_{\lambda_3\lambda_s}\delta_{\lambda_2\lambda_1}\delta(\mathbf{r}-\mathbf{r}_3)\,\delta(\mathbf{r}_2-\mathbf{r}_1)\,\delta(t_3)\,\delta(t_1).\end{aligned} \tag{A6}$$

APPENDIX B: CORRELATION-FUNCTION EXPRESSIONS FOR THE RESPONSE FUNCTIONS

Below we give explicit expressions for the first, second, and third order nonlinear response functions with combinations of ordinary (Hilbert space) correlation functions.

The linear response function [Eq. (A2)] may be written as

$$\mathsf{S}_{\lambda_1\lambda_s}(\mathbf{r};\mathbf{r}_1 t_1)=\mathsf{S}^{(1)}_I+\mathsf{S}^{(2)}_{II},$$

$$\mathsf{S}^{(1)}_I=\frac{i}{\hbar}\langle \hat{j}_{\lambda_s}(\mathbf{r},t_1)[\hat{j}_{\lambda_1}(\mathbf{r}_1,0),\rho(-\infty)]\rangle, \tag{B1}$$

$$\mathsf{S}^{(2)}_{II}=-\frac{e^2}{2mc}\langle \hat{\sigma}(\mathbf{r},0)\rho(-\infty)\rangle\,\delta(\mathbf{r},\mathbf{r}_1)\,\delta(t_1)\,\delta_{\lambda_s\lambda_1}.$$

The second order NRF [Eq. (A4)] is given by

$$\mathsf{S}^{(2)}_{\lambda_2\lambda_1\lambda_s}(\mathbf{r};\mathbf{r}_2\mathbf{r}_1 t_2 t_1)=\mathsf{S}^{(2)}_I+\mathsf{S}^{(2)}_{II}, \tag{B2}$$

$$\mathsf{S}^{(2)}_I=-\frac{1}{\hbar^2}\langle \hat{j}_{\lambda_s}(\mathbf{r},t_2+t_1)[\hat{j}_{\lambda_2}(\mathbf{r}_2,t_1),[\hat{j}_{\lambda_1}(\mathbf{r}_1,0),\rho(-\infty)]]\rangle,$$

$$\begin{aligned}\mathsf{S}^{(2)}_{II}=-\frac{i}{\hbar}\left(\frac{e^2}{2mc}\right)&\{\langle \hat{j}_{\lambda_s}(\mathbf{r},t_1)[\hat{\sigma}(\mathbf{r}_1,0),\rho(-\infty)]\rangle\,\delta_{\lambda_2\lambda_1}\\ &\times\delta(\mathbf{r}_2-\mathbf{r}_1)\,\delta(t_1)\\ &+\langle \hat{\sigma}(\mathbf{r},t_1)[\hat{j}_{\lambda_1}(\mathbf{r}_1,0),\rho(-\infty)]\rangle\,\delta_{\lambda_2\lambda_s}\\ &\times\delta(\mathbf{r}-\mathbf{r}_2)\,\delta(t_2)\}.\end{aligned}$$

The third order NRF [Eq. (A6)] is given by

$$\mathsf{S}^{(3)}_{\lambda_3\lambda_2\lambda_1\lambda_s}(\mathbf{r};\mathbf{r}_3\mathbf{r}_2\mathbf{r}_1 t_3 t_2 t_1)=\mathsf{S}^{(3)}_I+\mathsf{S}^{(3)}_{II}+\mathsf{S}^{(3)}_{III}, \tag{B3a}$$

$$\mathsf{S}_I^{(3)} = -\frac{i}{\hbar^3}\langle \hat{j}_{\lambda_s}(\mathbf{r},t_3+t_2+t_1)[\hat{j}_{\lambda_3}(\mathbf{r}_3,t_2+t_1),[\hat{j}_{\lambda_2}(\mathbf{r}_2,t_1),[\hat{j}_{\lambda_1}(\mathbf{r}_1,0),\rho(-\infty)]]]\rangle, \tag{B3b}$$

$$\begin{aligned}\mathsf{S}_{II}^{(3)} = \frac{1}{\hbar^2}\left(\frac{e^2}{2mc}\right)\{&\langle \hat{j}_{\lambda_s}(\mathbf{r},t_3+t_1)[\hat{\sigma}(\mathbf{r}_3,t_1)\\ &\times[\hat{j}_{\lambda_1}(\mathbf{r}_1,0),\rho(-\infty)]]\rangle \delta_{\lambda_2\lambda_3}\delta(\mathbf{r}_2-\mathbf{r}_3)\,\delta(t_2)\\ &+\langle \hat{j}_{\lambda_s}(\mathbf{r},t_3+t_2)[\hat{j}_{\lambda_3}(\mathbf{r}_3,t_2)[\hat{\sigma}(\mathbf{r}_2,0),\rho(-\infty)]]\rangle\\ &\times \delta_{\lambda_2\lambda_1}\delta(\mathbf{r}_2-\mathbf{r}_1)\,\delta(t_1)+\langle \hat{\sigma}(\mathbf{r},t_2+t_1)[\hat{j}_{\lambda_2}(\mathbf{r}_3,t_1)\\ &\times[\hat{j}_{\lambda_1}(\mathbf{r}_1,0),\rho(-\infty)]]\rangle \delta_{\lambda_2\lambda_1}\delta_{\lambda_3\lambda_s}\delta(\mathbf{r}-\mathbf{r}_3)\,\delta(t_3)\},\end{aligned} \tag{B3c}$$

$$\mathsf{S}_{III}^{(3)} = \frac{i}{\hbar}\left(\frac{e^2}{2mc}\right)^2 \langle \hat{\sigma}(\mathbf{r},t_2)[\hat{\sigma}(\mathbf{r}_2,0),\rho(-\infty)]\rangle \delta_{\lambda_3\lambda_s}\delta_{\lambda_2\lambda_1} \times \delta(\mathbf{r}-\mathbf{r}_3)\,\delta(\mathbf{r}_2-\mathbf{r}_1)\,\delta(t_3)\,\delta(t_1). \tag{B3d}$$

In the above equations, $\hat{j}_\lambda(\mathbf{r},t)$ and $\hat{\sigma}(\mathbf{r},t)$ are the current and charge density operators respectively, in the Heisenberg representation, i.e.,

$$\hat{j}_\lambda(\mathbf{r},t) \equiv \exp\left[\frac{i}{\hbar}H_0 t\right]\hat{j}_\lambda \exp\left[-\frac{i}{\hbar}H_0 t\right] \tag{B4}$$

and similarly for $\hat{\sigma}(\mathbf{r},t)$.

$\mathsf{S}^{(3)}$ has three contributions: four time correlation functions of current density [Eq. (B3a)], three time correlation functions of current density and charge density [Eq. (B3c)], and the two time correlation functions of the charge density [Eq. (B3d)].

APPENDIX C: NONLINEAR SUSCEPTIBILITIES IN THE FREQUENCY DOMAIN

Exact compact formal relations between $\mathcal{S}^{(n)}$ and $\mathsf{S}^{(n)}$ can be derived in the frequency domain. From Eq. (17), the relation of the Fourier components for the polarization and the current density is written as

$$\mathbf{P}(\mathbf{r},\omega) = \frac{i}{\omega}\mathbf{J}(\mathbf{r},\omega). \tag{C1}$$

Here the nonlinear response functions are replaced by the susceptibilities $\tilde{\mathcal{S}}^{(n)}$ defined as

$$P^{(n)}(\mathbf{r},\omega) = \frac{1}{(2\pi)^n}\int d\omega_1 \cdots \int d\omega_n \int d\mathbf{r}_1 \cdots \int d\mathbf{r}_n \tilde{\mathcal{S}}^{(n)}(\mathbf{r}\omega;\mathbf{r}_n,\ldots,\mathbf{r}_1,\omega_n,\ldots,\omega_1)\tilde{E}_1(\mathbf{r}_1\omega_1)\times\cdots\times\tilde{E}_n(\mathbf{r}_n\omega_n). \tag{C2}$$

These are connected to $\mathcal{S}^{(n)}$ via the Fourier transform

$$\begin{aligned}&\tilde{\mathcal{S}}^{(n)}(\mathbf{r}\omega;\mathbf{r}_n,\ldots,\mathbf{r}_1,\omega_n,\ldots,\omega_1)\\ &\quad = \int d\omega_1,\ldots,\int d\omega_n \mathcal{S}^{(n)}\mathbf{r};(\mathbf{r}_n,\ldots,\mathbf{r}_1,t_n\ldots t_1)\\ &\quad \times\exp[i\omega_1 t_1 + i(\omega_1+\omega_2)t_2+\cdots\\ &\quad + i(\omega_1+\omega_2+\cdots+\omega_n)t_n].\end{aligned} \tag{C3}$$

A similar definition can be introduced for the current/vector potential response functions [Eq. (12)]. Comparing with Eq. (C2) we get

$$\tilde{\mathcal{S}}^{(n)}(\mathbf{r}\omega;\mathbf{r}_n,\ldots,\mathbf{r}_1,\omega_n,\ldots,\omega_1) = \frac{i^{1-n}}{\omega_1\omega_2\cdots\omega_n\omega}\tilde{\mathsf{S}}^{(n)}(\mathbf{r}\omega;\mathbf{r}_n,\ldots,\mathbf{r}_1,\omega_n,\ldots,\omega_1). \tag{C4}$$

APPENDIX D: NRF'S FOR TRXD AND PUMP-PROBE TECHNIQUES

Below we present the explicit expressions for the NRF's for the TRXA [Eq. (29)] and the TRXD [Eq. (E8)] technqiues.

Equations (29) are recast in the forms

$$\begin{aligned}R_1 = -\mathrm{Tr}[&\hat{j}(\mathbf{r}_1)e^{(i/\hbar)H_0(t_1+t_2+t_3)}\hat{j}(\mathbf{r})e^{-(i/\hbar)H_0 t_3}\hat{j}(\mathbf{r}_3)\\ &\times e^{-(i/\hbar)H_0 t_2}\hat{j}(\mathbf{r}_2)e^{-(i/\hbar)H_0 t_1}\rho(-\infty)],\end{aligned} \tag{D1a}$$

$$\begin{aligned}R_2 = -\mathrm{Tr}[&e^{(i/\hbar)H_0 t_1}\hat{j}(\mathbf{r}_2)e^{(i/\hbar)H_0(t_2+t_3)}\hat{j}(\mathbf{r})e^{-(i/\hbar)H_0 t_3}\hat{j}(\mathbf{r}_3)\\ &\times e^{-(i/\hbar)H_0(t_2+t_1)}\hat{j}(\mathbf{r}_1)\rho(-\infty)],\end{aligned} \tag{D1b}$$

$$\begin{aligned}R_3 = \mathrm{Tr}[&\hat{j}(\mathbf{r}_1)e^{(i/\hbar)H_0 t_1}\hat{j}(\mathbf{r}_2)e^{(i/\hbar)H_0(t_2+t_3)}\hat{j}(\mathbf{r})e^{-(i/\hbar)H_0 t_3}\hat{j}(\mathbf{r}_3)\\ &\times e^{-(i/\hbar)H_0(t_2+t_1)}\rho(-\infty)],\end{aligned} \tag{D1c}$$

$$\begin{aligned}R_4 = \mathrm{Tr}[&e^{(i/\hbar)H_0(t_1+t_2+t_3)}\hat{j}(\mathbf{r})e^{-(i/\hbar)H_0 t_3}\hat{j}(\mathbf{r}_3)\\ &\times e^{-(i/\hbar)H_0 t_2}\hat{j}(\mathbf{r}_2)e^{-(i/\hbar)H_0 t_1}\hat{j}(\mathbf{r}_1)\rho(-\infty)].\end{aligned} \tag{D1d}$$

Equations (E8) are rewritten as follows:

$$R_1^{XD}=\mathrm{Tr}[e^{(i/\hbar)H_0t_1}\hat{j}(\mathbf{r}_2)e^{(i/\hbar)H_0t_2}\hat{\sigma}(\mathbf{r}_3)e^{(i/\hbar)H_0t_3}\hat{\sigma}(\mathbf{r}) \times e^{-(i/\hbar)H_0(t_3+t_2+t_1)}\hat{j}(\mathbf{r}_1)\rho(-\infty)], \tag{D2a}$$

$$R_2^{XD}=\mathrm{Tr}[\hat{j}(\mathbf{r}_1)e^{(i/\hbar)H_0(t_1+t_2)}\hat{\sigma}(\mathbf{r}_3)e^{(i/\hbar)H_0t_3}\hat{\sigma}(\mathbf{r}) \times e^{-(i/\hbar)H_0(t_3+t_2)}\hat{j}(\mathbf{r}_2)e^{-(i/\hbar)H_0t_1}\rho(-\infty)], \tag{D2b}$$

$$R_3^{XD}=-\mathrm{Tr}[\hat{j}(\mathbf{r}_1)e^{(i/\hbar)H_0t_1}\hat{j}(\mathbf{r}_2)e^{(i/\hbar)H_0t_2}\hat{\sigma}(\mathbf{r}_3) \times e^{(i/\hbar)H_0t_3}\hat{\sigma}(\mathbf{r})e^{-(i/\hbar)H_0(t_3+t_2+t_1)}\rho(-\infty)], \tag{D2c}$$

$$R_4^{XD}=-\mathrm{Tr}[e^{(i/\hbar)H_0(t_1+t_2)}\hat{\sigma}(\mathbf{r}_3)e^{(i/\hbar)H_0t_3}\hat{\sigma}(\mathbf{r}) \times e^{-(i/\hbar)H_0(t_3+t_2)}\hat{j}(\mathbf{r}_2)e^{-(i/\hbar)H_0t_1}\hat{j}(\mathbf{r}_1)\rho(-\infty)]. \tag{D2d}$$

APPENDIX E: TIME-RESOLVED X-RAY DIFFRACTION

In TRXD experiments the system is irradiated by the optical pump pulse, and then the x-ray probe pulse is scattered after a time delay τ. We assume that the frequency of the x-ray probe pulse is detuned far off resonance from any excitation of the material.

In this appendix we derive an expression for the TRXD signal in terms of the NRF's. As indicated in Sec. I, even though x-ray scattering intensity is proportional to the incident x-ray intensity, the process can be formulated as a nonlinear response. The apparent contradiction comes from the fact that the x-ray scattering process involves one strong incoming x-ray field and the scattered x-ray mode which has no photons initially. X-ray scattering can be viewed as a consequence of vacuum fluctuations of the x-ray radiation field. This mode, therefore, should be treated quantum mechanically, and unlike a classical field it does not show up in the signal through its amplitude [39].

We expand the vector potential as

$$A(\mathbf{r},t)=A_1(t+\tau)\exp[i(\mathbf{k}_1\cdot\mathbf{r}-\omega_1t)]+A_i(t) \times\exp[i(\mathbf{k}_i\cdot\mathbf{r}-\omega_it)]+A_s(t)\exp[i(\mathbf{k}_s\cdot\mathbf{r}-\omega_st)] +\text{c.c.}, \tag{E1}$$

where A_1, A_i, and A_s denote the optical pump, x-ray probe pulse, and scattered x-ray field, respectively. A_1 and A_2 are classical functions and only the scattered field is treated quantum mechanically, i.e.,

$$A_s=c\left(\frac{\epsilon_{\mathbf{q}_s}}{\omega_s}\right)b_s, \quad A_s^*=c\left(\frac{\epsilon_{\mathbf{q}_s}}{\omega_s}\right)b_s^\dagger. \tag{E2}$$

Hereafter, we will eliminate the polarization direction indices for simplicity.

The scattered x-ray field is initially in the vacuum state, so that its density operator is

$$|\rho_R(-\infty)\rangle\rangle=|n_S=0,n_S=0\rangle\rangle, \tag{E3}$$

and the total (material + field) initial density operator is given by

$$|\rho_T(-\infty)\rangle\rangle=|\rho(-\infty)\rangle\rangle|\rho_R(-\infty)\rangle\rangle, \tag{E4}$$

where $|\rho(-\infty)\rangle\rangle$ is the equilibrium material density operator.

The operator representing the photon emission rate is

$$\mathcal{N}_s\equiv\frac{d}{dt}b_s^+b_s=\frac{i}{\hbar}[H_{int},b_s^+b_s]. \tag{E5}$$

In TRXD the x-ray energies are far off resonance from any material excitation energies. We can thus neglect the H_1 contribution to Eq. (E5).

The time- and frequency-resolved photon emission rate is given by $\langle\langle\mathcal{N}_S|\rho(t)\rangle\rangle$. When $\rho_T(t)$ is expanded perturbatively in H_{int}, we find that the lowest order contribution to TRXD is third order in H_{int}. From Eq. (7), we obtain

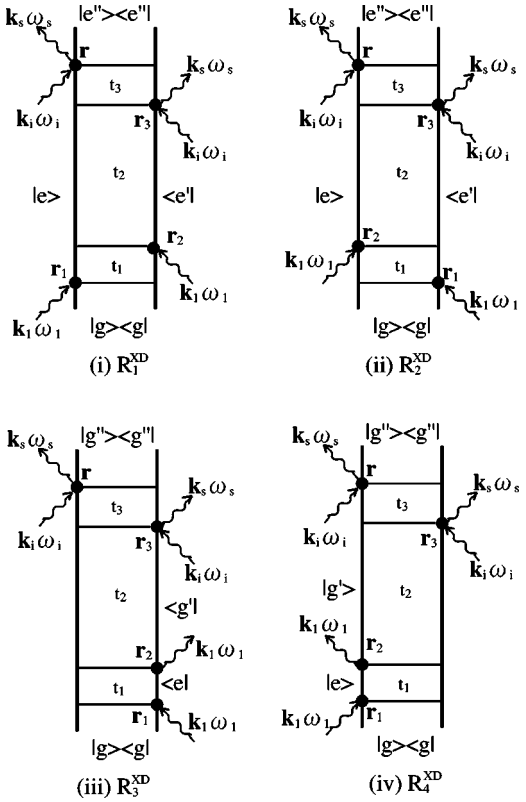

FIG. 2. Pictorial representation of the Liouville-space pathways contributing to the TRXD. Each pathway corresponds to the NRF of R_j^{XD} $(j=1-4)$ in Eqs. (24). g (or g') and e (or e') stand for the vibronic eigenstates of the ground and of the excited electronic states, respectively. When the pump pulse is in the optical region, e (or e') represent vibronic eigenstates of the optically excited state. When the pump pulse is in the x-ray region, e (or e') represent vibronic eigenstates of a core excited state.

$$\langle\langle \mathcal{N}_s|\rho^{(3)}(t)\rangle\rangle$$
$$= \frac{1}{\hbar^4}\int d\mathbf{r}\int d\mathbf{r}_3\int d\mathbf{r}_2\int d\mathbf{r}_1\int dt_3\int dt_2\int dt_1$$
$$\times\langle\langle b_s^\dagger b_s|\mathcal{L}_2(\mathbf{r},t)\mathcal{G}(t_3)\mathcal{L}_{int}(\mathbf{r}_3,t-t_3)\mathcal{G}(t_2)$$
$$\times\mathcal{L}_{int}(\mathbf{r}_2,t\quad -t_3-t_2)\mathcal{G}(t_1)\mathcal{L}_{int}(\mathbf{r}_1,t-t_3-t_2-t_1)$$
$$\times|\rho_T(-\infty)\rangle\rangle. \tag{E6}$$

We shall now apply this formula to calculate the TRXD for an optically excited two-electronic-level system. When the x-ray energies are far off resonance we need not specify the electronic levels for the x-ray excitation. Equation (E6) has many terms when evaluated, since each $\mathcal{L}_{int}$ is a commutator which can act either from the left or from the right, and can represent coupling with either the optical or the x-ray field modes. However, under the rotating-wave approximation, the number of these terms can be greatly reduced. Furthermore, we assume that the time delay τ of the x-ray probe pulse is long compared with any relaxation time scale of the material, so that coherent components in Eq. (E6) can be neglected. After integrating over t, the components of Eq. (E6) that survive the RWA are

$$W_{\mathrm{TRXD}}(\mathbf{k}_1\omega_1,\mathbf{k}_i\omega_i;\tau)=\int dt\langle\langle \mathcal{N}_s|\rho^{(3)}(t)\rangle\rangle$$
$$\propto 2\frac{1}{\omega_1^2\omega_i^2}\mathrm{Re}\int d\mathbf{r}\int d\mathbf{r}_3\int d\mathbf{r}_2\int d\mathbf{r}_1\int dt\int dt_3\int dt_2\int dt_1$$
$$\times\{E_1(t-t_3-t_2-t_1+\tau)E_1^*(t-t_3-t_2+\tau)E_i^*(t-t_3)E_i(t)$$
$$\times[R_1^{XD}(\mathbf{r};\mathbf{r}_3\mathbf{r}_2\mathbf{r}_1t_3t_2t_1)+R_4^{XD}(\mathbf{r};\mathbf{r}_3\mathbf{r}_2\mathbf{r}_1t_3t_2t_1)]\exp[-i\Delta\mathbf{k}\cdot(\mathbf{r}-\mathbf{r}_3)]\exp[i\omega_1t_1+i\Delta\omega t_3]\}$$
$$+\{E_1^*(t-t_3-t_2-t_1+\tau)E_1(t-t_3-t_2+\tau)E_i^*(t-t_3)E_i(t)[R_2^{XD}(\mathbf{r};\mathbf{r}_3\mathbf{r}_2\mathbf{r}_1t_3t_2t_1)$$
$$+R_3^{XD}(\mathbf{r};\mathbf{r}_3\mathbf{r}_2\mathbf{r}_1t_3t_2t_1)]\exp[-i\Delta\mathbf{k}\cdot(\mathbf{r}-\mathbf{r}_3)]\exp[-i\omega_1t_1+i\Delta\omega t_3]\}. \tag{E7}$$

The signal intensity is now represented by the electric field E rather than the vector potential A. This is done using the relation $\dot{A}=E$ and the slowly varying envelope approximation. In Eq. (E7), $\Delta\mathbf{k}\equiv\mathbf{k}_s-\mathbf{k}_i$ is the x-ray scattering wave vector and $\Delta\omega\equiv\omega_s-\omega_i$ is the energy loss. In the above expression we assumed the dipole approximation for the optical pump pulse and set $\mathbf{k}_1=\mathbf{0}$.

The Liouville-space pathways corresponding to these four terms are depicted in Fig. 2. The correlation functions R_j^{XD} $(j=1,\ldots,4)$ are written as

$$R_1^{XD}=\langle\hat{j}(\mathbf{r}_2,t_1)\hat{\sigma}(\mathbf{r}_3,t_1+t_2)\hat{\sigma}(\mathbf{r},t_1+t_2+t_3)\hat{j}(\mathbf{r}_1,0)\rangle, \tag{E8a}$$

$$R_2^{XD}=\langle\hat{j}(\mathbf{r}_1,0)\hat{\sigma}(\mathbf{r}_3,t_1+t_2)\hat{\sigma}(\mathbf{r},t_1+t_2+t_3)\hat{j}(\mathbf{r}_2,t_1)\rangle, \tag{E8b}$$

$$R_3^{XD}=-\langle\hat{j}(\mathbf{r}_1,0)\hat{j}(\mathbf{r}_2,t_1)\hat{\sigma}(\mathbf{r}_3,t_1+t_2)\hat{\sigma}(\mathbf{r},t_1+t_2+t_3)\rangle, \tag{E8c}$$

$$R_4^{XD}=-\langle\hat{\sigma}(\mathbf{r}_3,t_1+t_2)\hat{\sigma}(\mathbf{r},t_1+t_2+t_3)\hat{j}(\mathbf{r}_2,t_1)\hat{j}(\mathbf{r}_1,0)\rangle. \tag{E8d}$$

In the above expressions, $\hat{j}(\mathbf{r}_1,t)$ and $\hat{\sigma}(\mathbf{r},t)$ are the Heisenberg representations of the current density and the charge density operators, respectively. Explicit expressions in the correlation functions are listed in Appendix D. These correlation functions can also be written by the sum over eigenstates representation,

$$R_1^{XD} = \sum_{ge''e'e} P(g)\sigma_{e''e'}(\mathbf{r})\sigma^*_{e''e'}(\mathbf{r}_3)j^*_{e'g}(\mathbf{r}_2)j_{eg}(\mathbf{r}_1)I_{ee''}(t_3)I_{ee'}(t_2)I_{eg}(t_1), \tag{E9a}$$

$$R_2^{XD} = \sum_{ge''e'e} P(g)\sigma_{e''e}(\mathbf{r})\sigma^*_{e''e'}(\mathbf{r}_3)j_{eg}(\mathbf{r}_2)j^*_{e'g}(\mathbf{r}_1)I_{ee''}(t_3)I_{ee'}(t_2)I_{ge'}(t_1), \tag{E9b}$$

$$R_3^{XD} = -\sum_{gg''g'e} P(g)\sigma_{g''g}(\mathbf{r})\sigma^*_{g''g'}(\mathbf{r}_3)j^*_{g'e}(\mathbf{r}_2)j^*_{eg}(\mathbf{r}_1)I_{gg''}(t_3)I_{gg'}(t_2)I_{ge}(t_1), \tag{E9c}$$

$$R_4^{XD} = -\sum_{gg''g'e} P(g)\sigma_{g''g'}(\mathbf{r})\sigma^*_{g''g}(\mathbf{r}_3)j^*_{g'e}(\mathbf{r}_2)j^*_{eg}(\mathbf{r}_1)I_{g'g''}(t_3)I_{g'g}(t_2)I_{eg}(t_1), \tag{E9d}$$

where g and g' denote the vibronic eigenstates for the ground electronic state, and e or e' are vibronic states belonging to the optically excited electronic state. The population probability in the ground state is denoted by $P(g)$. $j_{\alpha\beta}$ and $\sigma_{\alpha\beta}$ $(\alpha,\beta = g,g',g'',e,e',e'')$ are the matrix elements of the current density and the charge density, respectively.

It should be noted that in the pathways for R_1^{XD} and R_2^{XD} the system is in the optically excited electronic state during the t_2 period, while in the R_3^{XD} and R_4^{XD} pathways it is in the ground electronic state.

[1] P. M. Rentzepis and J. Helliwell, *Time-Resolved Electron and X-ray Diffraction* (Oxford University Press, New York, 1995).

[2] J. Cao and K. R. Wilson, J. Phys. Chem. **102**, 9523 (1998).

[3] F. L. H. Brown, K. R. Wilson, and J. Cao, J. Chem. Phys. **111**, 6238 (1999).

[4] C. W. Siders, A. Cavalleri, K. Sokolowski-Tinten, C. S. Toth, T. Guo, M. Kammler, M. Horn von Hoegen, K. R. Wilson, D. van der Linde, and C. P. J. Barty, Science **286**, 1340 (1999).

[5] M. Ben-Nun, J. Cao, and K. R. Wilson, J. Phys. Chem. A **101**, 8743 (1997).

[6] M. Schnurer, C. Spielmann, P. Wobrauschek, C. Streli, N. H. Burnett, C. Kan, K. Ferencz, R. Koppitsch, Z. Cheng, T. Brabec, and F. Krausz, Phys. Rev. Lett. **80**, 3236 (1998).

[7] G. Steinmeyer, D. H. Sutter, L. Gallmann, N. Matuschek, and U. Keller, Science **286**, 1507 (1999).

[8] I. V. Tomov, D. A. Oulianov, P. Chen, and P. M. Rentzepis, J. Phys. Chem. B **103**, 7081 (1999).

[9] A. H. Chin, R. W. Sconenlein, T. E. Glover, P. Baling, W. P. Leemans, and C. V. Shank, Phys. Rev. Lett. **83**, 336 (1999).

[10] B. Perman, S. Anderson, M. Schmidt, and K. Moffat, Cell Mol. Biol. (Oxford) **46**, 895 (2000); K. Moffat, Acta Crystallogr., Sect. A: Found. Crystallogr. **54**, 833 (1998); V. Srajer, T. Y. Teng, T. Ursby, C. Prodervand, Z. Ren, S. Adachi, W. Schildkamp, D. Bourgeois, M. Wulff, and K. Moffat, Science **274**, 1726 (1996).

[11] C. Bressler, M. Chergui, P. Pattison, M. Wulff, A. Flipponi, and R. Abela, Proc. SPIE **3451**, 108 (1998); C. Bressler, M. Saes, M. Chergui, R. Abela, and P. Pattison, Nucl. Instrum. Methods Phys. Res. (to be published); Ch. Bressler, M. Saes, M. Chergui, R. Abela, and P. Pattison (unpublished).

[12] F. Raksi, K. R. Wilson, Z. Jiang, A. Ikhlef, C. Y. Cote, and J. C. Kieffer, J. Chem. Phys. **104**, 6066 (1996).

[13] R. W. Schoenlein, S. Chattopadhyay, H. H. W. Chong, T. E. Glover, P. A. Heimann, C. V. Shank, A. A. Zholents, and M. S. Zolotorev, Science **287**, 223 (2000).

[14] C. R. Petruck, T. Guo, R. Jimenez, F. Raksi, J. A. Squier, B. C. Walker, K. R. Wilson, and C. P. J. Barty, Proc. SPIE **3157**, 84 (1997).

[15] M. Ben-Nun, T. J. Martinez, P. M. Weber, and K. R. Wilson, Chem. Phys. Lett. **262**, 405 (1996).

[16] F. Raksi, K. R. Wilson, Z. Jiang, A. Ikhlef, C. Y. Cote, and J-C. Kieffer, Proc. SPIE **2523**, 306 (1995).

[17] C. R. Petruck, R. Jimenez, T. Guo, A. Cavalleri, C. W. Siders, F. Raski, J. A. Squier, B. C. Walker, K. R. Wilson, and C. P. J. Barty, Nature (London) **398**, 310 (1999).

[18] I. V. Tomov, P. Chen, and P. M. Rentzepis, Rev. Sci. Instrum. **66**, 5214 (1995).

[19] D. J. Segel, A. Bachmann, J. Hofrichter, K. O. Hodgson, S. Doniach, and T. Kiefhaber, J. Mol. Biol. **288**, 489 (1999); L. L. Chen, G. Wildegger, T. Kiefhaber, K. O. Hodgson, and S. Doniach, *ibid.* **276**, 225 (1998).

[20] J. J. Rehr and R. C. Albers, Rev. Mod. Phys. **72**, 621 (2000).

[21] D. C. Koningsberger, *X-Ray Absorption: Principles, Applications, Techniques of EXAFS, SEXAFS, and XANES* (Wiley, New York, 1988).

[22] Y. Ma, K. E. Miyano, P. L. Cowan, Y. Aglitzkiy, and B. A. Karlin, Phys. Rev. Lett. **74**, 478 (1995).

[23] Y. Murakami, J. P. Hill, D. Gibbs, M. Blume, I. Koyama, M. Tanaka, H. Kawata, T. Arima, Y. Tokura, K. Hirota, and Y. Endoh, Phys. Rev. Lett. **81**, 582 (1998).

[24] K. Hamalainen, J. P. Hill, S. Huotari, C.-C. Kao, L. E. Berman, A. Kotani, T. Ide, J. L. Peng, and R. L. Greene, Phys. Rev. B **61**, 1836 (2000).

[25] Y. Tezuka, S. Shin, A. Agui, M. Fujisana, and T. Ishii, J. Phys. Soc. Jpn. **65**, 312 (1996).

[26] J. Nordgren, P. Glans, K. Gunnelin, J. Guo, P. Skytt, C. Sather, and N. Wassdahl, Appl. Phys. A: Mater. Sci. Process. **65**, 97 (1997).

[27] A. Cesar, F. Gel'mukhanov, Y. Luo, H. Agren, P. Skytt, P. Glans, J. Guo, K. Gunnelin, and J. Nordgren, J. Chem. Phys. **106**, 3439 (1997).

[28] M. Magnuson, L. Yang, J.-H. Guo, C. Sathe, A. Agui, J. Nordgren, Y. Luo, A. Agren, N. Hohansson, W. R. Salancek, L. E.

Horsburgh, and A. P. Monkman, Chem. Phys. **237**, 295 (1998).
[29] A. Kotani, J. Phys. Chem. **61**, 419 (2000); J. Electron Spectrosc. Relat. Phenom. **92**, 171 (1997); S. Tanaka and A. Kotani, J. Phys. Soc. Jpn. **62**, 464 (1993).
[30] E. Pahl, H. D. Meyer, and L. S. Cederbaum, Z. Phys. D: At., Mol. Clusters **38**, 215 (1996); L. S. Cederbaum and F. Tarantelli, J. Chem. Phys. **99**, 5871 (1993); E. Pahl, J. Brand, and L. S. Cederbaum, Phys. Rev. A **60**, 1079 (1999).
[31] P. M. Platzman and E. D. Isaacs, Phys. Rev. B **57**, 11 107 (1998).
[32] M. van Veenendaal, P. Carra, and B. T. Thole, Phys. Rev. B **54**, 16 010 (1996).
[33] Y. Ma, Phys. Rev. B **49**, 5799 (1994).
[34] F. Gelmnkhanov and H. Agren, Phys. Rev. A **54**, 379 (1996).
[35] S. Tanaka, Y. Kayanuma, and K. Ueda, Phys. Rev. A **57**, 3437 (1998).
[36] K. Ueda, J. Electron Spectrosc. Relat. Phenom. **88-91**, 1 (1998).
[37] M. Simon, C. Miron, N. Leclercq, P. Morin, K. Ueda, Y. Sato, S. Tanaka, and Y. Kayanuma, Phys. Rev. Lett. **79**, 3857 (1997).
[38] K. Ueda, S. Tanaka, Y. Shimizu, Y. Muramatsu, H. Chiba, T. Hayaishi, M. Kitajima, and H. Tanaka, Phys. Rev. Lett. **85**, 3129 (2000).
[39] S. Mukamel, *Principles of Nonlinear Spectroscopies* (Oxford University Press, New York, 1995).
[40] T. S. Rose, R. Righini, and M. D. Fayer, Chem. Phys. Lett. **106**, 13 (1984).
[41] J. Knoester and S. Mukamel, Phys. Rep. **205**, 1 (1991).
[42] H. J. Eichler, P. Gunter, and D. W. Pohl, *Laser-Induced Dynamic Gratings* (Springer, Berlin, 1986).
[43] E. A. Power, *Introductory Quantum Electrodynamics* (Longmans, London, 1964); D. P. Craig and T. Thirunamachandran, *Molecular Quantum Dynamics* (Academic Press, London, 1984); E. A. Power, Adv. Chem. Phys. **12**, 167 (1967).
[44] B. W. Shore, *The Theory of Coherent Atomic Excitations* (Wiley, New York, 1990), Vol. 1.
[45] V. Chernyak and S. Mukamel, Phys. Rev. B **48**, 2470 (1993).
[46] V. Chernyak and S. Mukamel, J. Chem. Phys. **100**, 2974 (1994).
[47] V. Chernyak, N. Wang, and S. Mukamel, Phys. Rep. **263**, 213 (1995).
[48] V. Chernyak and S. Mukamel, Chem. Phys. **198**, 133 (1995).
[49] G. D. Mahan, Phys. Rev. **153**, 882 (1967); **163**, 612 (1967).
[50] P. Nozieres and C. T. deDominicis, Phys. Rev. **178**, 1097 (1969).
[51] O. Gunnarsson and K. Schonhammer, Phys. Rev. B **28**, 4315 (1983).
[52] A. Kotani and Y. Toyozawa, J. Phys. Soc. Jpn. **35**, 1073 (1973).
[53] J. C. Williamson and A. H. Zewail, J. Phys. Chem. **98**, 2766 (1994).
[54] V. Chernyak, S. N. Volkov, and S. Mukamel (unpublished).
[55] S. A. Malinovskaya and L. S. Cederbaum, Phys. Rev. A **61**, 042706 (2000).
[56] Y. Ma and M. Blume, Rev. Sci. Instrum. **66**, 1543 (1995).
[57] J. P. Hannon, G. T. Trammell, M. Blume, and D. Gibbs, Phys. Rev. Lett. **61**, 1245 (1988).
[58] M. Blume, J. Appl. Phys. **57**, 3615 (1985).
[59] S. Ishihara and S. Maekawa, Phys. Rev. Lett. **80**, 3799 (1998).
[60] Y. Murakami, H. Kawada, H. Kawata, M. Tanaka, T. Arima, Y. Moritomo, and Y. Tokura, Phys. Rev. Lett. **80**, 1932 (1998).
[61] K. D. Finkelstein, Q. Shen, and S. Shastri, Phys. Rev. Lett. **69**, 1612 (1992).
[62] D. H. Templeton and L. K. Templeton, Phys. Rev. B **49**, 14 850 (1994).
[63] D. H. Templeton and L. K. Templeton, Acta Crystallogr., Sect. A: Cryst. Phys., Diffr., Theor. Gen. Crystallogr. **38**, 62 (1982).
[64] F. Gel'mukhanov, P. Salek, A. Shalagin, and H. Agren, J. Chem. Phys. **112**, 5593 (2000).
[65] T. Takagi, Y. Kayanuma, and S. Tanaka, J. Phys. Soc. Jpn. **68**, 434 (1999); F. Gel'mukhanov and H. Ågren, Phys. Rep. **312**, 87 (1999).